



**UNIVERSITY
OF TRENTO**

DEPARTMENT OF INFORMATION AND COMMUNICATION TECHNOLOGY

38050 Povo – Trento (Italy), Via Sommarive 14
<http://www.dit.unitn.it>

**SYNTHESIS OF A THREE-DIMENSIONAL TRIBAND (L1-L2 GPS AND
WI-FI) PREFRACTAL TREE ANTENNA**

R. Azaro, E. Zeni, T. Gazzini, R. Dallapiccola, A. Massa

November 2006

Technical Report DIT-06-068

Synthesis of a Three-Dimensional Triband (*L1-L2 GPS* and *Wi-Fi*) Prefractal Tree Antenna

Renzo Azaro, *Member, IEEE*, Edoardo Zeni, Tommaso Gazzini, Ramona Dallapiccola,
Andrea Massa, *Member, IEEE*

Department of Information and Communication Technologies,

University of Trento, Via Sommarive 14, 38050 Trento - Italy

Tel. +39 0461 882057, Fax +39 0461 882093

E-mail: andrea.massa@ing.unitn.it, {[renzo.azaro](mailto:renzo.azaro@dit.unitn.it), [edoardo.zeni](mailto:edoardo.zeni@dit.unitn.it)}@dit.unitn.it

Web: <http://www.eledia.ing.unitn.it>

Synthesis of a Three-Dimensional Triband (*L1-L2 GPS* and *Wi-Fi*) Prefractal Tree Antenna

Renzo Azaro, *Member, IEEE*, Edoardo Zeni, Tommaso Gazzini, Ramona Dallapiccola, Andrea Massa, *Member, IEEE*

Abstract

In this letter, the synthesis of a 3D wire antenna with a tree-like shape and operating at three different frequency bands (*L1 – L2 GPS* bands and *Wi – Fi*) is presented. The geometrical parameters of the antenna are determined by means of a particle swarm-based optimization procedure exploiting the degrees of freedom of the reference tree geometry for fitting the electrical project constraints. The results of the numerical simulation are shown and compared with those from experimental measurements for assessing the effectiveness of the synthesis procedure.

Key Words - Antennas Synthesis, Fractal Antennas, Tree-like Antennas, Multiband Antennas, Particle Swarm Optimizer.

1 Introduction

Because of the growing demand of miniaturized and multiband antennas for electronic devices employing multiple wireless standards, several researches have been devoted at analyzing the electrodynamic behavior of fractal and pre-fractal geometries [1] [2] [3]. As a matter of fact, fractal and pre-fractal geometries present very interesting features in terms of multiband behavior and overall size.

Besides planar geometries [4][5][6], easily built on dielectric substrates by means of standard and low-cost photolithographic techniques, three-dimensional fractal tree-like shapes have been investigated [7]. As a matter of fact, despite their complex realization, these structures present very interesting electrodynamic properties thanks to the large number of degrees of freedom in the choice of the values of their descriptive geometric parameters. In [7], *Petko and Werner* showed that fractal tree geometries can be fruitfully employed as end-loads for the miniaturization of conventional dipoles or monopole antennas.

However, although a multi-band behavior can be realized, the spectral distribution of multiple resonant frequencies is strictly related to the geometrical parameters of the self-similar structure with fixed relationships among the frequencies whatever the fractal shape. Therefore, the allocation of several working frequency bands in the frequency spectrum turns out to be a complex task with “*constrained*” choices. In order to overcome such a limitation, the insertion of reactive loads in the fractal tree structure has been proposed in [7] at the cost of an increased complexity in the construction process of the device.

Another effective methodology for obtaining a multiband behavior, without constraints on resonance frequencies, is based on the introduction of perturbations both in size and length of the fractal geometry [8][9][10][11]. According to this guideline, this paper presents the design of a three-dimensional pre-fractal tree antenna operating at three different frequency bands (*GPS* L_1 - L_2 bands and *Wi-Fi*). The synthesis of the pre-fractal geometry is carried out through a numerical optimization procedure based on a particle swarm optimizer (*PSO*) [12][13][14], which optimizes the geometrical parameters describing the tree geometry avoiding the insertion of any lumped load to obtain a multiband behavior. The effectiveness of the design procedure and the characteristics of the synthesized three-

dimensional triband antenna are analyzed by means of representative numerical results and measurements on an experimental prototype.

2 Triband Pre-Fractal Tree Antenna Design and Optimization

The synthesis of the three-dimensional geometry of the multiband prefractal tree has been formulated as an optimization problem by fixing suitable constraints in terms of gain values and impedance matching at the input port (*Return Loss* values) in both L_1 and L_2 frequency bands of the *GPS* system (centered respectively at $f_1 = 1575.42$ MHz and at $f_2 = 1227.60$ MHz) as well as in the *Wi-Fi* band (centered at $f_3 = 2440.00$ MHz).

As far as the impedance matching is concerned, a Return Loss lower than -10 dB is required. Moreover, the radiation characteristics of the three-dimensional antenna are required to satisfy the following constraints. Concerning L_1 and L_2 *GPS* bands, an hemispherical coverage is needed with gain values suitable for commercial *GPS* receivers. More in detail, gain values greater than $G_{min} = 3.0$ dBi at $\theta = 0^\circ$ and greater than $G_{min} = -4.0$ dBi at $\theta = 70^\circ$ by assuming the presence of a low noise 30 dB preamplifier stage at the input port of the *GPS* receiver because of the weakness of the *GPS* signals at the earth surface. Furthermore, taking into account the performances required by a commercial mobile transmitter/receiver in the *Wi-Fi* band, the following constraints have been defined: gain values greater than $G_{min} = -6.0$ dBi at $\theta = 70^\circ$ and an average gain greater than $G_{minav} = -10.0$ dBi in the angular range $70^\circ < \theta < 90^\circ$. Finally, in order to minimize the overall size of the antenna, the 3D structure is required to belong to a volume having dimensions $\frac{\lambda_0}{4} \times \frac{\lambda_0}{4} \times \frac{\lambda_0}{4}$, being $\frac{\lambda_0}{4} \cong 6$ cm at the lowest resonance frequency ($f_2 = 1227.60$ MHz).

According to [7][15], the self similar structure of the prefractal tree has been derived by repeatedly applying the so-called Hutchinson operator up to the stage $i = 3$. As shown in Fig. 1, starting from a trunk of length l_0 lying along the z -axis in a cartesian coordinate system [Fig. 1(a)], the fractal tree structure is generated by the iterative addition of

junctions from which several branches (called *child* branches) split from a *parent* branch. Except the trunk and the final branches, every branch is connected to a junction at its own terminations. Thus, it is at the same time child and parent of other branches. These structures can be grouped in different classes depending on: (a) the number of branches R that lead off a junction, (b) the bent angle ξ_b with respect to the parent direction, and (c) the angle ξ_s that separates the consecutive branches leading off the same junction. In this paper, in order to simplify the building procedure, a four branches ($R = 4$) fractal tree characterized by $\xi_b = 90^\circ$ and $\xi_s = 90^\circ$ has been considered. Therefore, the resulting fractal shape is composed by branches lying along the axes of the coordinate system and the antenna structure is uniquely determined by: (i) the trunk length l_0 and (ii) the lengths $l_{i,j}$ of the branches, i being the iteration index and j ($j = 1, \dots, R^i$) denotes the j -th branch generated at the i -th stage ($i = 1, \dots, I$) as pictorially shown in Fig. 1(b) ($i = 1$), Fig. 1(c) ($i = 2$), and Fig. 1(d) ($i = 3$). Summarizing, the I -th order prefractal tree is constituted by $L = \sum_{i=1}^I R^{(I-i+1)} + 1$ segments (the branches and the trunk) of circular cross-section $r = 0.5 \text{ mm}$ in radius.

Under these assumptions, the descriptive parameters of the pre-fractal tree (trunked at $I = 3$ for tuning three different resonance frequencies) have been optimized by minimizing the following cost function

$$\mathfrak{S}(\underline{\gamma}) = \sum_{m=0}^{M-1} \sum_{n=0}^{N-1} \sum_{t=0}^{T-1} \left\{ \max \left[0, \frac{G_{min} \{t\Delta\theta, n\Delta\phi, m\Delta f\} - \Phi \{t\Delta\theta, n\Delta\phi, m\Delta f\}}{G_{min}} \right] \right\} \quad (1)$$

$$+ \sum_{v=0}^{V-1} \left\{ \max \left[0, \frac{\Psi \{v\Delta f\} - VSWR_{max}}{VSWR_{max}} \right] \right\}$$

where $\underline{\gamma} = \{l_0, l_{i,j}, i = 1, \dots, I = 3, j = 1, \dots, R^i\}$, Δf is the sampling frequency step in the $L1$, $L2$ and $Wi - Fi$ bands, $\Delta\theta$ and $\Delta\phi$ are the sampling angular steps of the gain function, $\Phi \{\underline{\gamma}\} = \Phi \{t\Delta\theta, n\Delta\phi, m\Delta f\}$ is the gain function of the radiating structure $\underline{\gamma}$ computed at $(\theta = t\Delta\theta, \phi = n\Delta\phi, f = m\Delta f)$, and $\Psi \{\underline{\gamma}\} = \Psi \{v\Delta f\}$ is the $VSWR$ value at $f = m\Delta f$. Moreover, since besides electrical constraints some other conditions have been stated for limiting the physical size of the antenna, a set of geometrical constraints have been defined to avoid the synthesis of unfeasible structures.

According to the guidelines described in [13], a suitable implementation of the PSO

[16] has been integrated with a tree-like prefractal generator and a method-of-moments (*MoM*) electromagnetic simulator [17] for minimizing (1), thus determining the antenna structure. More in detail, starting from the trial solutions $\underline{\gamma}_p^{(k)}$ ($p \in [1, P]$ and $k \in [1, K]$ being the index of the particle in the solutions swarm and the iteration index, respectively) iteratively generated by the *PSO*, the prefractal generator determines the corresponding antenna structure. Then, the *VSWR* and gain values are computed by means of the *MoM* simulator, which takes into account the presence of a reference ground plane of infinite extent. The iterative process continues until $k = K$ or $\mathfrak{S}^{opt} \leq \eta$, η being the convergence threshold and $\mathfrak{S}^{opt} = \min_k \left\{ \min_p \left[\mathfrak{S} \left(\underline{\gamma}_p^{(k)} \right) \right] \right\}$.

3 Numerical Analysis and Experimental Validation

Concerning the *PSO* implementation, the following setup has been used: a swarm of $P = 8$ trial solutions, a threshold $\eta = 10^{-3}$, and a maximum number of iterations equal to $K = 2000$. The remaining *PSO* parameters have been set taking into account the guidelines proposed in [13] and according to the rules defined in [16].

As an illustrative example of the optimization process, Fig. 2 shows the evolution of the behaviors of the *VSWR* in correspondence with the optimal solution determined at successive iterations of the optimization process. As it can be observed, starting from a completely mismatched configuration ($k = 0$), the solution improves ($k = 10$, $k = 50$) until an antenna design is found ($k = k_{conv}$) that fits the electrical specifications. As far as the geometric constraints are concerned, the synthesized structure turns out to be adequate since its maximum dimensions are equal to 3.28 [mm] along the x -axis, 5.17 [mm] along the y -axis, and 3.82 [mm] along the z -axis.

From the computational point of view, Figure 3 shows the plot of the optimal value of the cost function \mathfrak{S}^{opt} versus the iteration number k . As it can be noticed, the optimization required $k_{conv} = 75$ with a *CPU*-time at each iteration of about 5 sec (*Pentium IV*, 1800 MHz, 512 MB RAM).

Thanks to the solution estimated at the end of the *PSO*-based optimization, a prototype of the three-dimensional antenna has been built (Fig. 4). In order to carry out the experimental assessment, the trunk of the tree has been soldered to an *SMA* con-

necter previously assembled on a reference ground plane whose dimensions was equal to $90 \times 140 [cm^2]$ and the Return Loss values have been measured with a scalar network analyzer by placing the measurement setup inside an anechoic chamber. Figure 5 shows a comparison between computed and measured values that points out a satisfactory agreement among simulations and experiments.

A similar comparative evaluation has also been performed for the radiation properties of the antenna. More in detail, Figure 6 shows measured and simulated gain functions in the horizontal plane [$\theta = 0^\circ$ - Fig. 6(a)] and in a vertical plane [$\phi = 0^\circ$ - Fig. 6(b)]. As required, the antenna prototype allows an hemispherical coverage in the L_1 - L_2 *GPS* bands and, considering the 30 *dB* preamplification stage at the input port, the gain values turn out to be compliant with the requirements ($\Phi_{GPS} \{\theta = 0^\circ\} > G_{min} \{\theta = 0^\circ\} = 3 \text{ dBi}$ and $\Phi_{GPS} \{\theta = 70^\circ\} > G_{min} \{\theta = 70^\circ\} = -4 \text{ dBi}$). Similar conclusions hold true for the *Wi-Fi* frequency band ($\Phi_{Wi-Fi} \{\theta = 70^\circ\} > G_{min} \{\theta = 70^\circ\} = -6 \text{ dBi}$ and $\Phi_{AvGPS} \{70^\circ < \theta < 90^\circ\} > G_{min Av} \{70^\circ < \theta < 90^\circ\} = -3 \text{ dBi}$).

4 Conclusions

The design and the optimization of a three-dimensional triband prefractal tree antenna has been described. The antenna structure has been synthesized by optimizing the lengths of the branches of a prefractal tree with a suitable particle swarm-based algorithm in order to comply with geometrical and electrical requirements. A prototype of the triband antenna has been built and an exhaustive set of comparisons between measured and simulated antenna parameters has been carried out.

Acknowledgments

This work has been supported in Italy by the “*Progettazione di un Livello Fisico ‘Intelligente’ per Reti Mobili ad Elevata Riconfigurabilità,*” Progetto di Ricerca di Interesse Nazionale - MIUR Project COFIN 2005099984.

References

- [1] D. H. Werner and R. Mittra, *Frontiers in electromagnetics*. Piscataway: IEEE Press, 2000.
- [2] J. Gianvittorio and Y. Rahmat-Samii, "Fractals antennas: a novel antenna miniaturization technique, and applications," *IEEE Antennas Propagat. Mag.*, vol. 44, pp. 20-36, Feb. 2002.
- [3] D. H. Werner, R. L. Haupt, and P. L. Werner, "Fractal antenna engineering: the theory and design of fractal antenna arrays," *IEEE Antennas Propagat. Mag.*, vol. 41, pp. 37-59, Oct. 1999.
- [4] M. Sindou, G. Ablart, and C. Sourdois, "Multiband and wideband properties of printed fractal branched antennas," *Electron. Lett.*, vol. 35, no. 3, pp. 181-182, Feb. 1999.
- [5] C. Puente, J. Claret, F. Sangues, J. Romeu, M.Q. Lopez-Salvans, and R. Pous, "Multiband properties of a fractal tree antenna generated by electrochemical deposition," *Electron. Lett.*, vol. 32, no. 25, pp. 2298-2299, Dec. 1996.
- [6] D. H. Werner, A. R. Bretones, and B. R. Long, "Radiation characteristics of thin-wire ternary fractal trees," *Electron. Lett.*, vol. 35, no. 8, pp. 609-610, Dec. 1999.
- [7] J. S. Petko and D. H. Werner, "Miniature reconfigurable three-dimensional fractal tree antennas," *IEEE Trans. Antennas Propagat.*, vol. 52, no. 8, pp. 1945-1956, Aug. 2004.
- [8] C. Puente, J. Romeu, R. Pous, X. Garcia, and F. Benitez, "Fractal multiband antenna based on the Sierpinski gasket," *Electron. Lett.*, vol. 32, pp. 1-2, Jan. 1996.
- [9] M. Fernandez Pantoja, F. Garcia Ruiz, A. Rubio Bretones, R. Gomez Martin, J. M. Gonzales-Arbesù, J. Romeu, and J. M. Rius, "GA design of wire pre-fractal antennas and comparison with other euclidean geometries," *IEEE Antennas Wireless Propagat. Lett.*, vol. 2, pp. 238-241, 2003.

- [10] M. Fernandez Pantoja, F. Garcia Ruiz, A. Rubio Bretones, S. Gonzales Garcia, R. Gomez Martin, J. M. Gonzales-Arbesù, J. Romeu, J. M. Rius, P. L. Werner, and D. H. Werner, "GA design of small thin-wire antennas: comparison with Sierpinski type prefractal antennas," *IEEE Trans. Antennas Propagat.*, vol. 54, pp. 1879-1882, Jun. 2006.
- [11] R. Azaro, F. De Natale, M. Donelli, E. Zeni, and A. Massa, "Synthesis of a prefractal dual-band monopolar antenna for GPS applications," *IEEE Antennas Wireless Propagat. Lett.*, vol. 5, pp. 361-364, 2006.
- [12] J. Kennedy, R. C. Eberhart, and Y. Shi, *Swarm Intelligence*. San Francisco: Morgan Kaufmann Publishers, 2001.
- [13] J. Robinson and Y. Rahmat-Samii, "Particle swarm optimization in electromagnetics," *IEEE Trans. Antennas Propagat.*, vol. 52, pp. 397-407, Feb. 2004.
- [14] M. Donelli and A. Massa, "A computational approach based on a particle swarm optimizer for microwave imaging of two-dimensional dielectric scatterers," *IEEE Trans. Microwave Theory Techn.*, vol. 53, pp. 1761-1776, May 2005.
- [15] D. H. Werner, P. L. Werner, and D. H. Church, "Genetically engineered multiband fractal antennas," *Electron. Lett.*, vol. 37, pp. 1150-1151, Sep. 2001.
- [16] R. Azaro, F. De Natale, M. Donelli, A. Massa, and E. Zeni, "Optimized design of a multi-function/multi-band antenna for automotive rescue systems," *IEEE Trans. Antennas Propagat.*, vol. 54, no. 2, pp. 392-400, Feb. 2006.
- [17] R. F. Harrington, *Field Computation by Moment Methods*. Malabar, Florida: Robert E. Krieger Publishing Co., 1987.

Figure Captions

- **Figure 1.** Geometry of the Tri-Band Prefractal Tree Antenna: (a) $i = 0$, (b) $i = 1$, (c) $i = 2$, and (d) $i = I = 3$.
- **Figure 2.** Simulated Return Loss at the input port of the Tri-Band Prefractal Tree Antenna at different iterations of the optimization process: (a) $k = 0$, (b) $k = 10$, (c) $k = 50$, and (d) $k = k_{conv}$.
- **Figure 3.** Behavior of the cost function versus the iteration number.
- **Figure 4.** Photograph of the prototype of the Tri-Band Prefractal Tree Antenna.
- **Figure 5.** Comparison between measured and simulated Return Loss values.
- **Figure 6.** Computed and measured values of the gain function in the (a) horizontal plane ($\theta = 0^\circ$) and in the (b) vertical plane ($\phi = 0^\circ$).

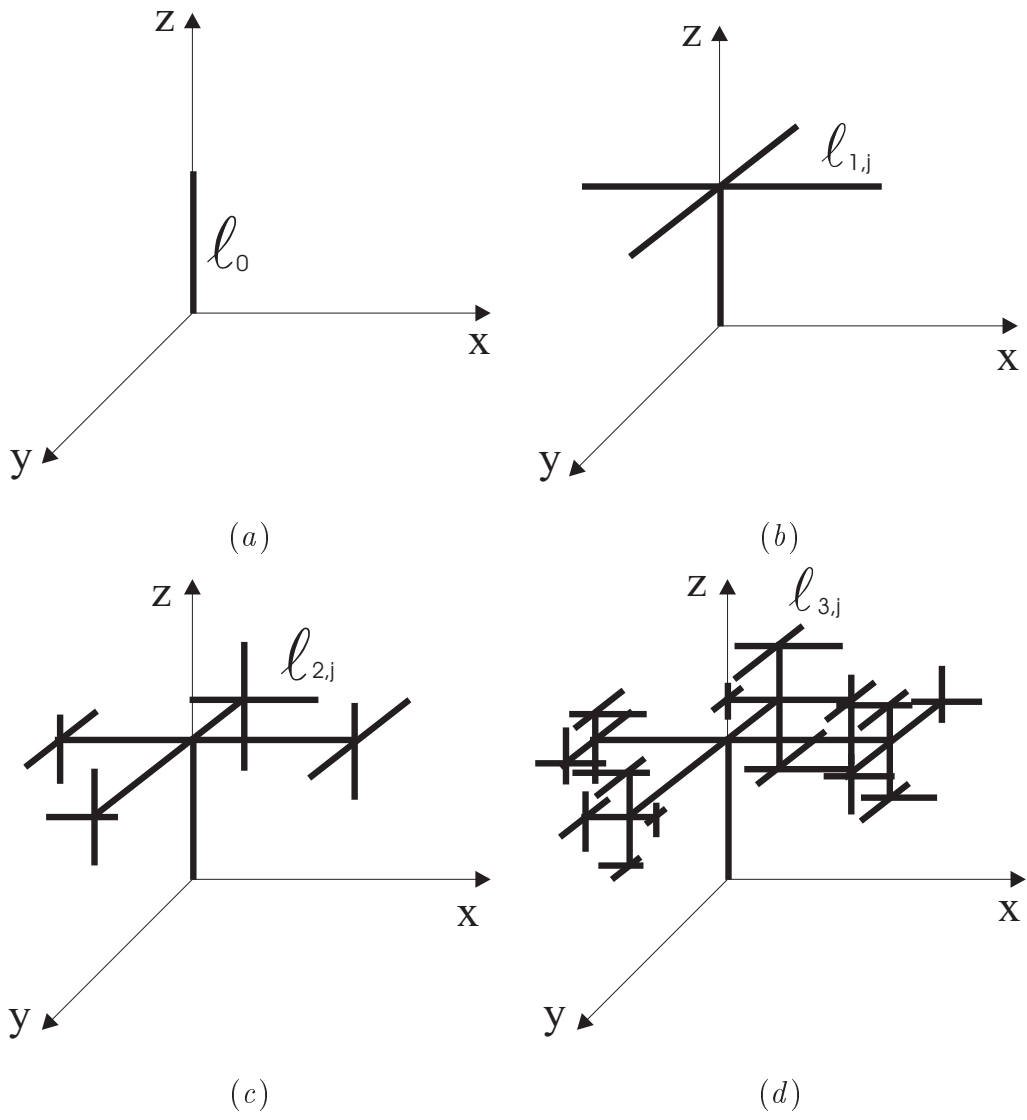


Figure 1 - R. Azaro *et al.*, "Synthesis of a three-dimensional triband ..."

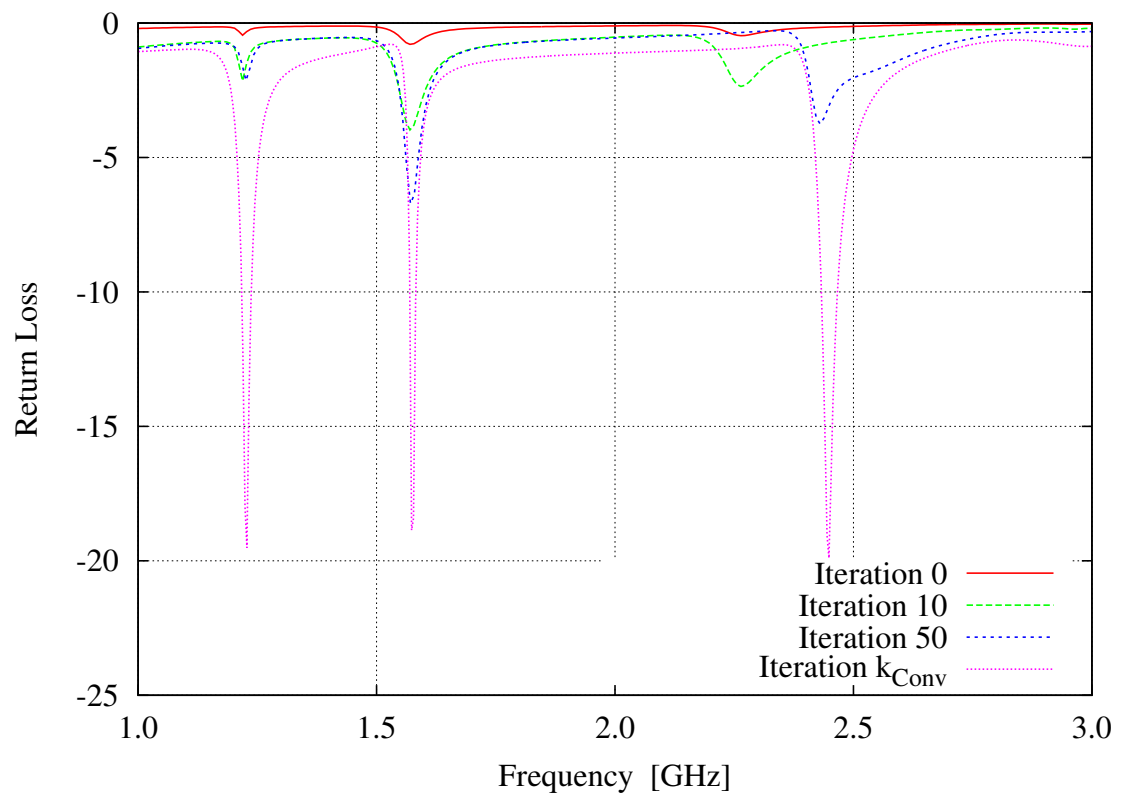


Figure 2 - R. Azaro *et al.*, "Synthesis of a three-dimensional triband ..."

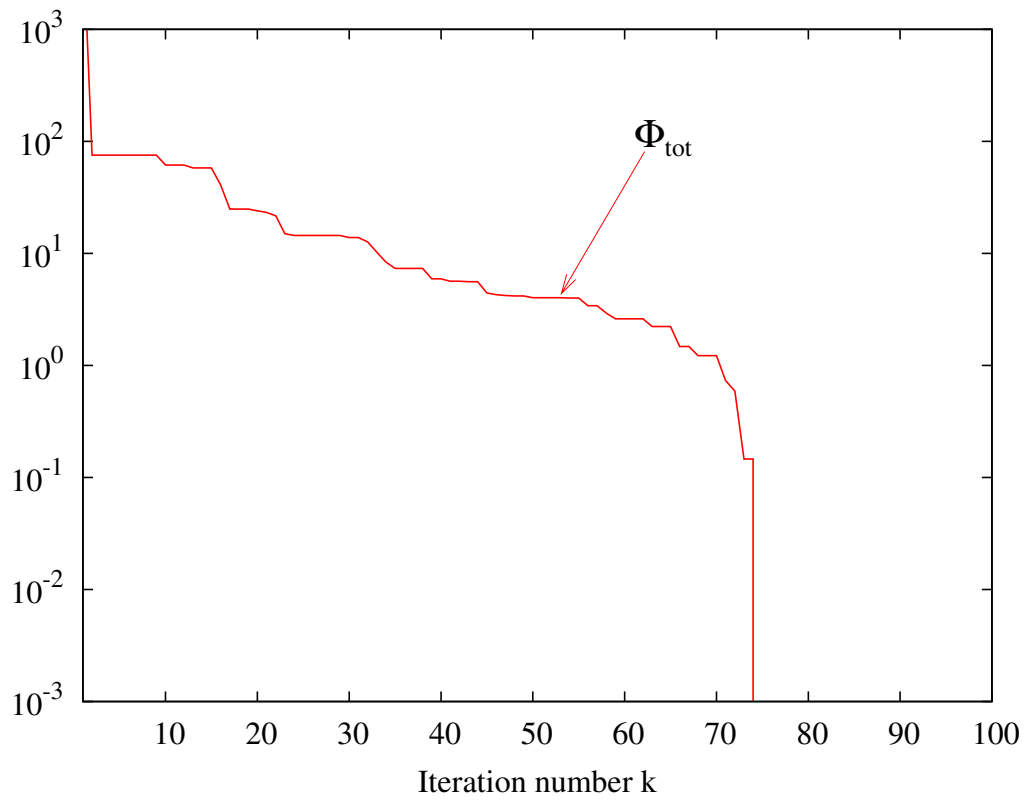


Figure 3 - R. Azaro *et al.*, "Synthesis of a three-dimensional triband ..."

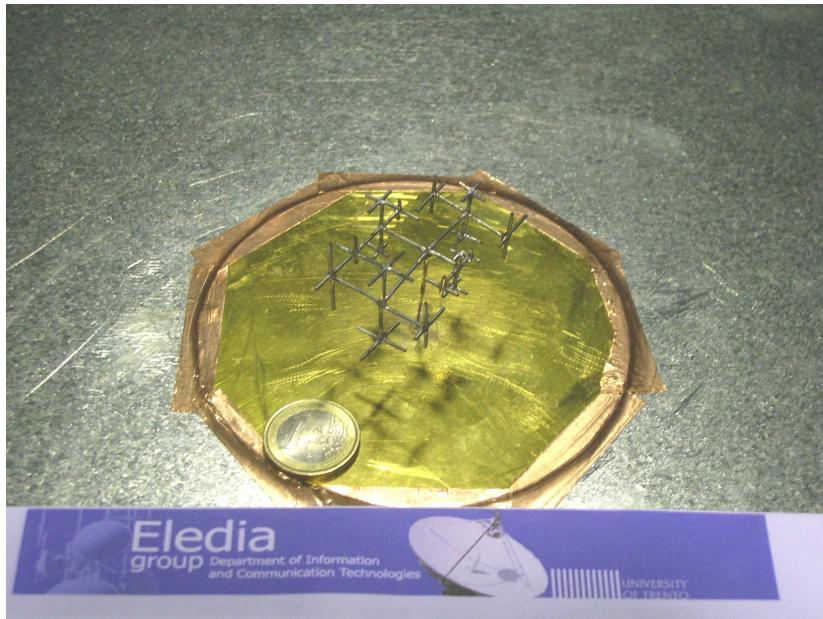


Figure 4 - R. Azaro *et al.*, "Synthesis of a three-dimensional triband ..."

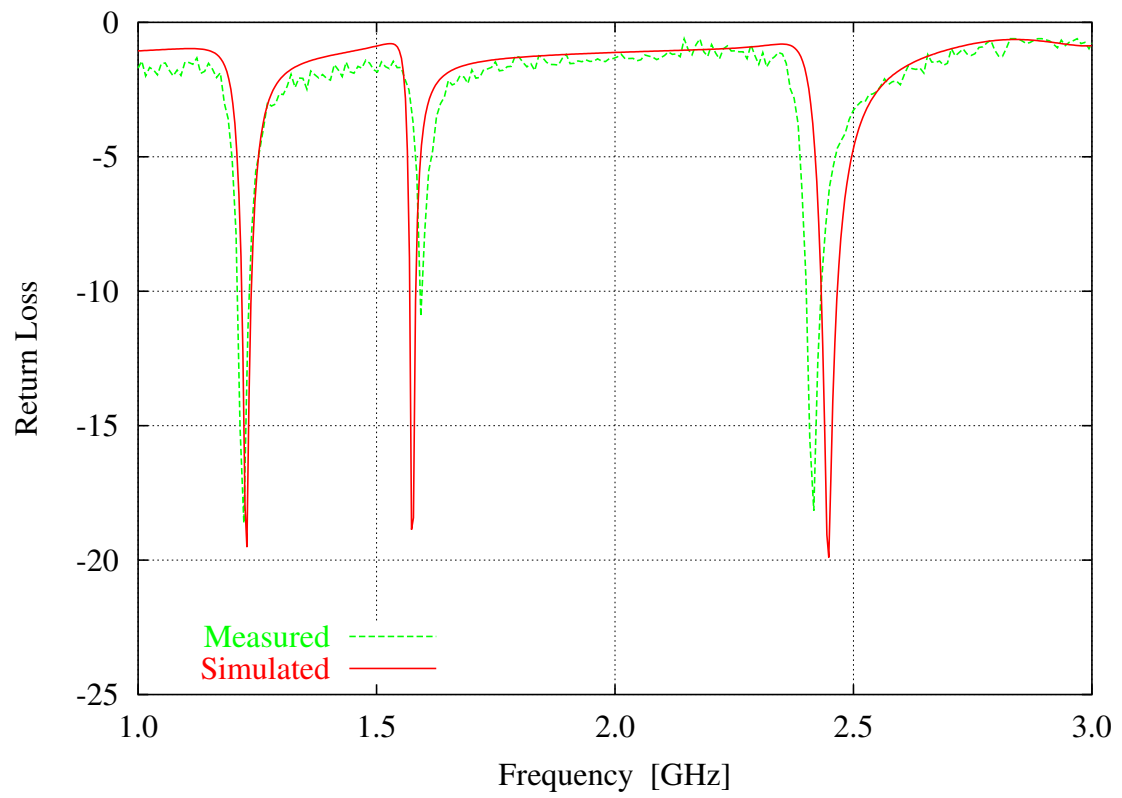
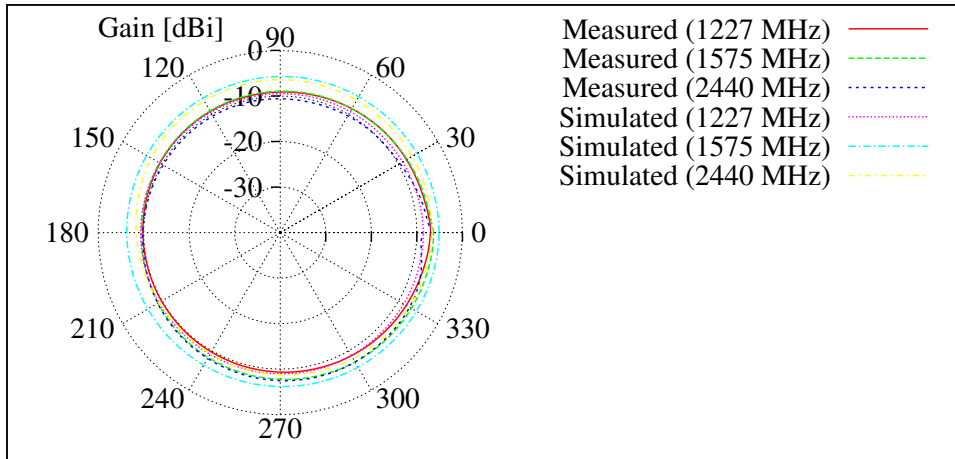
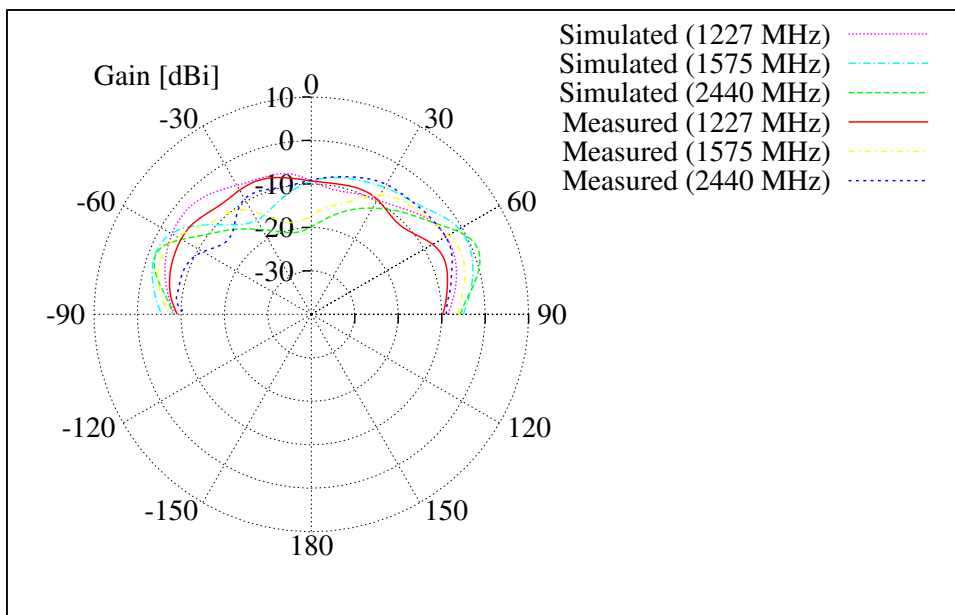


Figure 5 - R. Azaro *et al.*, "Synthesis of a three-dimensional triband ..."



(a)



(b)

Figure 6 - R. Azaro *et al.*, "Synthesis of a three-dimensional triband ..."